



# Climatology of mixed layer depth in the Gulf of Aden derived from in situ temperature profiles

Cheriyeri P. Abdulla<sup>1</sup> · Mohammed A. Alsaafani<sup>1,2</sup> · Turki M. Alraddadi<sup>1</sup> · Alaa M. Albarakati<sup>1</sup>

Received: 24 February 2018 / Revised: 5 February 2019 / Accepted: 15 February 2019 / Published online: 19 March 2019  
© The Oceanographic Society of Japan and Springer Nature Singapore Pte Ltd. 2019

## Abstract

For the first time in the Gulf of Aden, the climatology of mixed layer depth (MLD) is derived from in situ profiles of temperature at a spatial resolution of  $0.5^\circ \times 0.5^\circ$ . The climatology has captured all major features of the MLD variability in the Gulf of Aden. Deepening of the mixed layer is noticed during December–February associated with surface heat loss and cooling induced by strong convection. Further, the heat gain during March–May and subsequent warming strengthens the stratification and results in diminished mixing. The westward-moving cyclonic and anticyclonic eddies during winter change the mixed layer, especially along the northern and western Gulf of Aden. The observed permanent anticyclonic eddy during summer in the central part of the Gulf of Aden induces an additional deepening of the MLD by 30–40 m, even in the presence of a relatively strong stratification. The presence of nearly uniform north-easterly winds from October to April makes the MLD of the northern Gulf of Aden greater than the southern side during this period, while the south-westerly winds from June to August reverse the scenario and makes the northern Gulf of Aden shallower than the southern side.

**Keywords** Mixed layer depth · Climatology · Gulf of Aden · Upwelling · Eddies · Ekman transport

## 1 Introduction

The mixed layer is a striking and nearly universal ocean surface layer, generated by mixing associated with several processes including wind turbulence, surface cooling, wave breaking, current shear, and eddies. This layer is characterized by a quasi-uniform temperature and salinity. The detailed information about the thickness of this layer often referred to as the mixed layer depth, or MLD, is crucial in understanding the physical and biological processes in the upper ocean (Kara et al. 2003; de Boyer et al. 2004). The MLD variability has a strong impact on the distribution of heat (Chen et al. 1994), ocean biology (Polovina et al. 1995)

and near-surface acoustic propagation (Sutton et al. 2014), and it has been widely investigated over the years, both globally (Kara et al. 2003; de Boyer et al. 2004; Lorbacher et al. 2006) and regionally (D’Ortenzio et al. 2005; Lim et al. 2012; Keerthi et al. 2016). Wind-induced turbulence, warming or cooling in the surface layer associated with air–sea heat exchange, and the change in surface layer density by precipitation or evaporation are the primary forces influencing MLD variability.

The Gulf of Aden (hereafter “Gulf”) is one of the important marginal seas, through which the warm and highly saline Red Sea water is distributed to the Indian Ocean. Furthermore, the Gulf is one of the most productive areas with upwelling along both northern and southern coastal regions (Kabanova 1968; Currie et al. 1973; Yao and Hoteit 2015) and is a very busy economically important shipping route. It is an elongated stretch of water with length 900 km, area around  $220 \times 10^3 \text{ km}^2$  and an average depth of 1800 m which extends from the narrow strait of Bab-el-Mandab in the west up to the line that joins Ras-Fartak and Cape Guardafui in the east (Fig. 1). The region is strongly influenced by seasonally reversing monsoon winds with south-westerlies from June to August and north-easterlies from October to April, while May and September are transition months (Al

---

**Electronic supplementary material** The online version of this article (<https://doi.org/10.1007/s10872-019-00506-9>) contains supplementary material, which is available to authorized users.

---

✉ Cheriyeri P. Abdulla  
acp@stu.kau.edu.sa

<sup>1</sup> Department of Marine Physics, Faculty of Marine Sciences, King Abdulaziz University, Jeddah, Saudi Arabia

<sup>2</sup> Department of Earth and Environmental Sciences, Faculty of Science, Sana’a University, Sana’a, Yemen

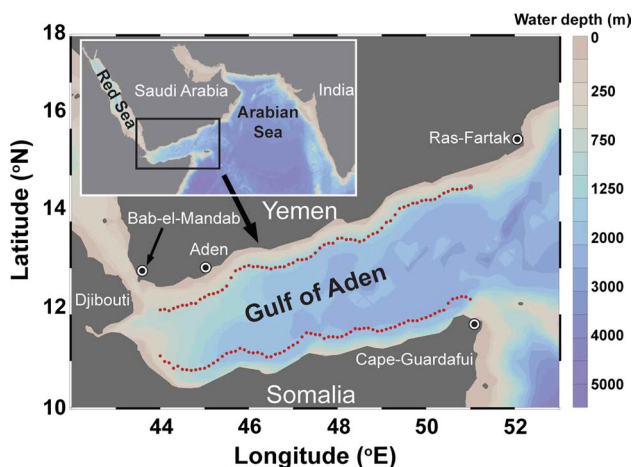


**Fig. 1** The geographical map of the Gulf of Aden. The red-dotted curves denote the coastal sections used in Fig. 11

Saafani and Shenoi 2007; Murray and Johns 1997; Smeed 1997). Circulation and hydrographic changes are largely forced by seasonal changes in wind pattern (Alsaafani et al. 2007). Further, the presence of frequent eddies throughout the year leads to a complex structure in both hydrography and circulation.

The available information on spatial and temporal changes of the mixed layer is sparse in the Gulf, which is vital for understanding the upper layer bio-physical processes. There is only one study reported so far, in which the MLD characteristics during February and August are described based on data from two cruises (Abdulla et al. 2016). Hence, the present study is motivated to introduce a monthly climatology of the MLD for the first time in the Gulf based on in situ observations and discusses the main physical processes. The sections are arranged as follows. Section 2 gives a brief description of the data sets and methods used for the present analysis. Section 3 discusses the variability of the MLD, the role of the heat and freshwater fluxes and the wind stress on MLD variability, the impact of eddies on MLD structure, and the shoaling of the mixed layer along the coast. Concluding remarks are given in the final section.

## 2 Data and methods

### 2.1 In situ profiles

Temperature and salinity profiles were downloaded from public data centers including the World Ocean Database [WOD, <https://www.nodc.noaa.gov/OC5/SELECT/dbsearch/dbsearch.html>], (Boyer et al. 2013)], Japan Oceanographic Data Center [JODC, <http://jdoss1.jodc.go.jp/vpage/>

scalar.html (J-DOSS 2003)] and Coriolis Data Center [CDC, <http://www.coriolis.eu.org/Data-Products/Data-Delivery/Data-selection> (Cabanes et al. 2013)]. Along with these profiles, profiles from different cruises are also used in the analysis. The data span from the year 1944 to 2017. They include profiles measured using a conductivity-temperature-density (CTD) profiler, autonomous profiling floats (PFLs) including ARGO floats, an expendable bathythermograph (XBT) and a mechanical bathythermograph (MBT). The XBT and MBT profiles are corrected based on Cheng et al. (2014).

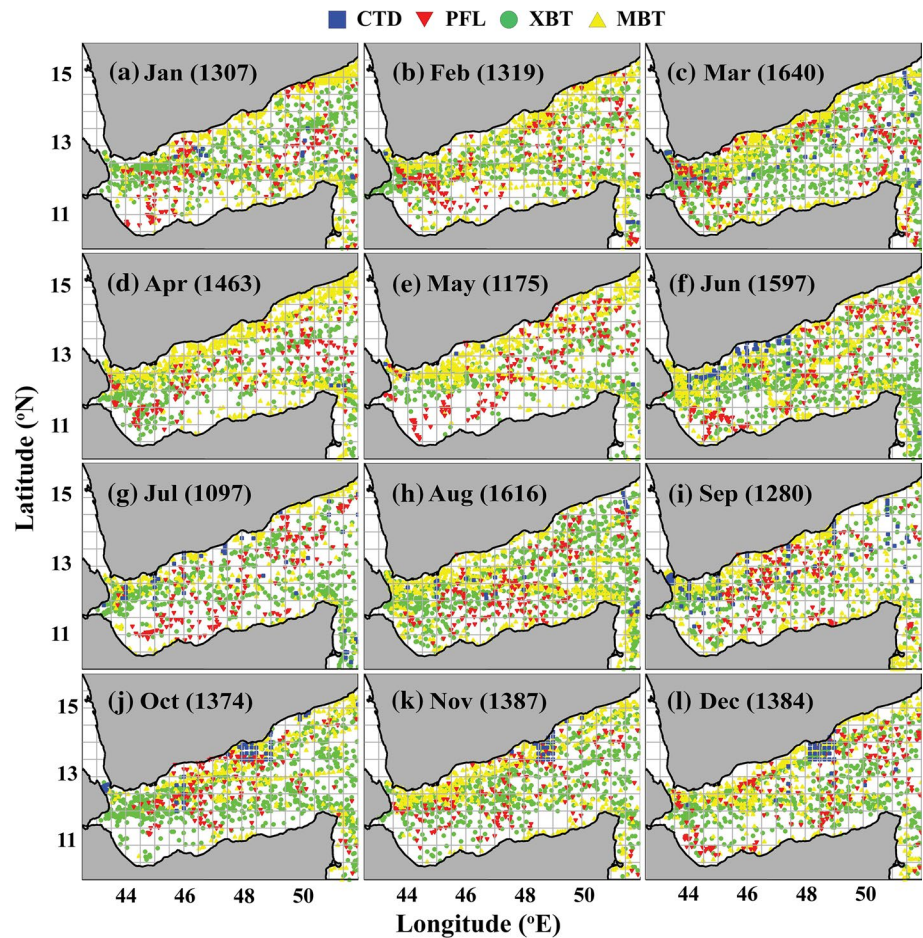
Altogether, 19,538 temperature and 2279 salinity profiles were collected in the Gulf from different sources. The number of salinity profiles is significantly lower (~ 14%) than the temperature profiles and sparse in both space and time. Further, no significant difference is noticed between the temperature-based MLD and that derived from density in the Gulf (Abdulla et al. 2016). Therefore, the salinity profiles are not included in the preparation of MLD climatology. The temperature profiles are quality-checked according to the procedure given in Boyer and Levitus 1994, and the number of profiles removed at each step of the quality check is tabulated in Table S1. The profiles in the Gulf, except those from the western Gulf, are considered unacceptable when the vertical temperature gradient derived from temperature at two adjacent levels is greater than  $0.3\text{ }^{\circ}\text{C m}^{-1}$ . The western Gulf profiles can display natural temperature inversions due to the large influx of Red Sea water. Therefore, the profiles with inversions are permitted in the western Gulf. In the duplicate check, when multiple profiles are available from the same station within 24 h, only the first profile of the day is included in the main dataset.

A total of 2627 profiles are removed from the main dataset during the quality check. After the quality control, a sum of 16,911 temperature profiles is available for the analysis, which includes profiles from CTD (984), PFL (1882), XBT (7488) and MBT (6557). The spread of available profiles is shown in Fig. 2. The monthly and yearly distribution of the profiles are given in the supplementary material (Figs. S1, S2 and S3).

### 2.2 Satellite datasets

Sea level anomaly (SLA) data is provided by AVISO ([www.avisioceanobs.com](http://www.avisioceanobs.com)) on daily to monthly scales. It is a merged product of satellite estimates from TOPEX/Poseidon, Jason-1, ERS-1/2, and Envisat and globally available for every  $0.25^{\circ} \times 0.25^{\circ}$  from the year 1992 to present (Le Traon and Dibarboure 1999; Ducet et al. 2000). Wind speed and direction are available from the Quick Scatterometer (QuikSCAT), an active microwave radar designed to measure electromagnetic backscatter from the wind-roughened ocean surface, for the period 1999–2009 (<http://apdrc.soest>

**Fig. 2** The monthly spread of temperature profiles in the Gulf of Aden



[.hawaii.edu/las/v6/constrain?var=13065](http://hawaii.edu/las/v6/constrain?var=13065)) and  $0.25^\circ \times 0.25^\circ$  spatial resolution (Wentz and Smith 2005). Precipitation estimates from the Tropical Rainfall Measuring Mission (TRMM; <https://pmm.nasa.gov/data-access/downloads/trmm>) are used to understand the amount of freshwater input to the Gulf, which is available for the period 1997–2015 with a spatial resolution of  $0.25^\circ \times 0.25^\circ$  (Huffman et al. 2007).

### 2.3 Reanalysis data

The monthly mean values of net heat flux (NHF) were downloaded from Tropflux ([http://www.incois.gov.in/tropflux\\_datasets/data/monthly/](http://www.incois.gov.in/tropflux_datasets/data/monthly/)) for the period from 1979 to 2017 and with a spatial resolution of  $1^\circ \times 1^\circ$  (Praveen Kumar et al. 2012). Tropflux is mainly derived from a combination of re-analysis data (from ERA-Interim for turbulent and longwave fluxes) and in situ measurements (from ISCCP for shortwave flux).

### 2.4 Methods

MLD for each profile is estimated based on the segment method (Abdulla et al. 2016, 2018). This method identifies

MLD with the help of standard deviation, gradient and curvature of the profile. The MLD estimates based on segment method are found to be less sensitive to short-range disturbances within the mixed layer, and are more reliable than commonly used approaches like threshold, gradient and curvature methods.

To prepare the monthly climatology of MLD, first, the individual MLD instances in each  $0.5^\circ \times 0.5^\circ$  grids were averaged separately for each month. Then, each individual MLD was compared with the averaged value, and those with a difference from average MLD greater than two standard deviations were removed. In the Gulf, approximately 90% of the grids have a minimum of three or more profiles, while the remaining 10% have no data or the number of profiles is less than three. We excluded the grids with less than three profiles during the objective analysis. Following de Boyer et al. (2004), a slight smoothing was applied based on a two-dimensional smoothing operator, that uses 50% weight for 8 neighboring grids and 50% self-weight. During this process, an additional weight was applied which depends on the number of available measurements in each grid box, where the grid boxes with more than 10 profiles were given ~100% confidence and those with three profiles

were given a confidence of  $\sim 10\%$ . Comparing to the simple linear interpolation, the smoothing based on weightage to the number of profiles improved the climatology (de Boyer et al. 2004; Terray 1994). The resultant smoothing equation is,

$$\text{MLD}_{i0'} = \frac{1}{\sum w_i} * \sum_{i \text{ neighboring } i0} (w_i * \text{MLD}_i) \quad (1)$$

$$w_i = \begin{cases} 8 * f(n_{i0}), & i = i0 \\ f(n_i), & i \neq i0 \end{cases} \quad (2)$$

$$f(n) = \left[ 1 - e^{-\frac{n^2}{4n_0}} \right] \quad (3)$$

where  $w_i$  is the smooth operator,  $n_i$  is the number of profiles in grid box  $i$ ,  $n_{i0}$  is the number of profiles in grid box  $i0$ , and  $n_0 = 10$ . The grids with no data were filled using an ordinary kriging method, which has been widely used as an optimal prediction technique in spatial data analysis (de Boyer et al. 2004; Wackernagel 1998). For the ease of explanation, the Gulf is subdivided into western (west of  $46^\circ\text{E}$ ),

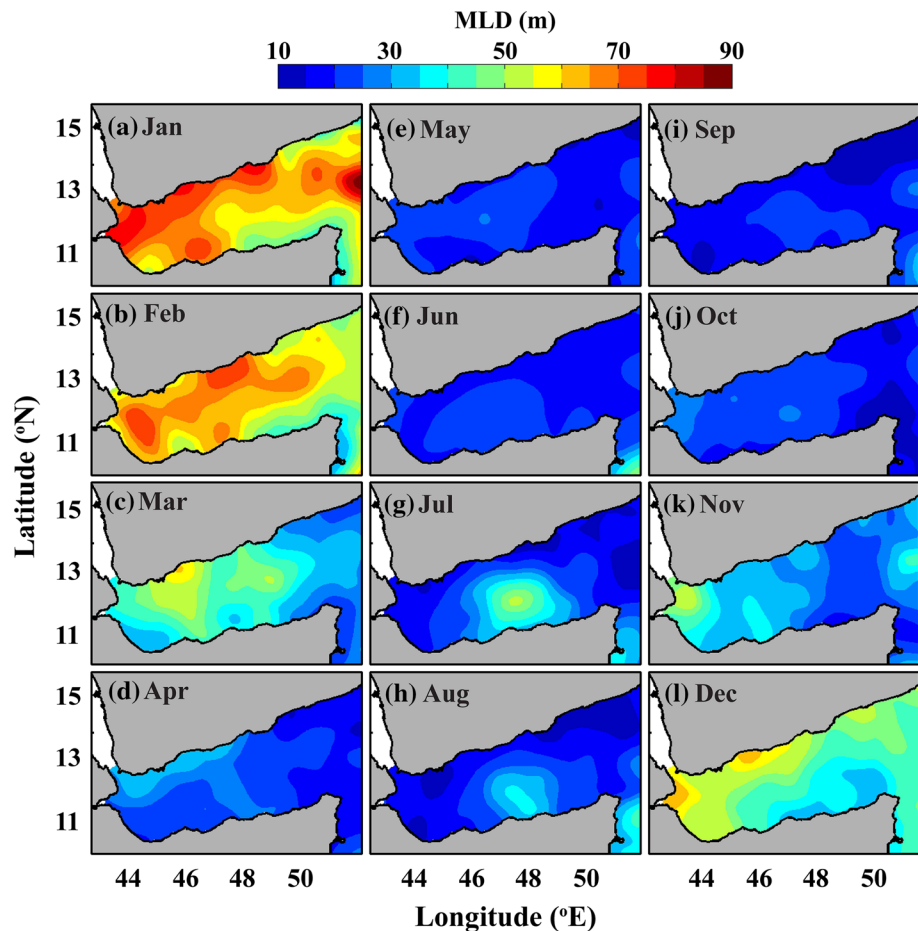
central ( $46^\circ\text{E}$ – $49^\circ\text{E}$ ) and eastern (east of  $49^\circ\text{E}$ ) regions, and the seasons are considered as winter (November–February), spring (March–May), summer (June–August) and fall (September–October).

### 3 Results and discussion

#### 3.1 Spatial and temporal variability of MLD in the Gulf of Aden

The monthly climatology of MLD in the Gulf of Aden, derived from in situ temperature profiles at a spatial resolution of  $0.5^\circ \times 0.5^\circ$ , is shown in Fig. 3. The winter deepening of the mixed layer commenced in the western Gulf in November (compared to October, approximately 20-m increase in MLD is noticed near the Bab-el-Mandab Strait), and then spread along the northern Gulf. Deepening of the mixed layer spread to other areas of the basin and displayed a mixed layer greater by  $\sim 40$  m in the western and northern Gulf in December. The winter deepening appeared almost in the entire basin by January and continued in February. The transition from deep to shallow MLD took place during

**Fig. 3** The monthly MLD climatology in the Gulf of Aden





March–April (average MLD difference from February to April is  $-37$  m). The shoaling is relatively rapid in the eastern and the southern part of the Gulf. The entire basin displayed a considerably shallower MLD from late spring to early fall (from April to October) for most of the region, except the central Gulf.

In contrast to the general summer mixed layer structure, the central Gulf experienced a greater MLD core during July–August, which is nearly 30–40 m deeper than the east and west of the Gulf. This difference is due to the presence of a permanent anticyclonic eddy in the central Gulf, which is discussed in detail in Sect. 3.3. The reverse process of transition from a shallow to a deep mixed layer took place during October–November.

During winter, the mixed layer in the western Gulf is 15–25 m deeper than the rest of the region, while the southern coast, especially in the central and eastern Gulf, experienced relatively shallow MLD. The transition from a deep to a shallow MLD is accomplished by March for the eastern Gulf, but is delayed to April for the central and western Gulf. The summer shoaling of the mixed layer is similar in both eastern and western basins with a significantly greater MLD in the central Gulf.

Previous study has shown that D20 (depth of 20 °C isotherm) is significantly greater in the western Gulf in February and in the central Gulf in August (Yao and Hoteit 2015), which is consistent with results from the MLD climatology introduced from this work. In comparison with the previous study by Abdulla et al. (2016), the climatological MLDs are shallower by  $< 10$  m, obviously due to the averaging of individual MLD values. The reported main features (the eastward MLD shoaling, the central summer deepening and the deep winter convection in the western Gulf) are clearly captured in the MLD climatology.

The MLD derived from in situ MLD temperature (MLDT) profiles is also compared with that derived from MLD density (MLDD) profiles; the difference between MLDT and MLDD is shown in Fig. 4. The available density profiles are limited to a few grid boxes, and the number of profiles is relatively less comparing to that of temperature profiles. The average difference between MLDT and MLDD (Table 1) is small compared to the depth of the mixed layer of the respective months.

The mixed layer temperature (MLT) is estimated from individual profiles. The spatially averaged MLT for the western, central and eastern Gulf are shown in Fig. 5. The

**Fig. 4** The difference between MLDT and MLDD (MLDT-MLDD)

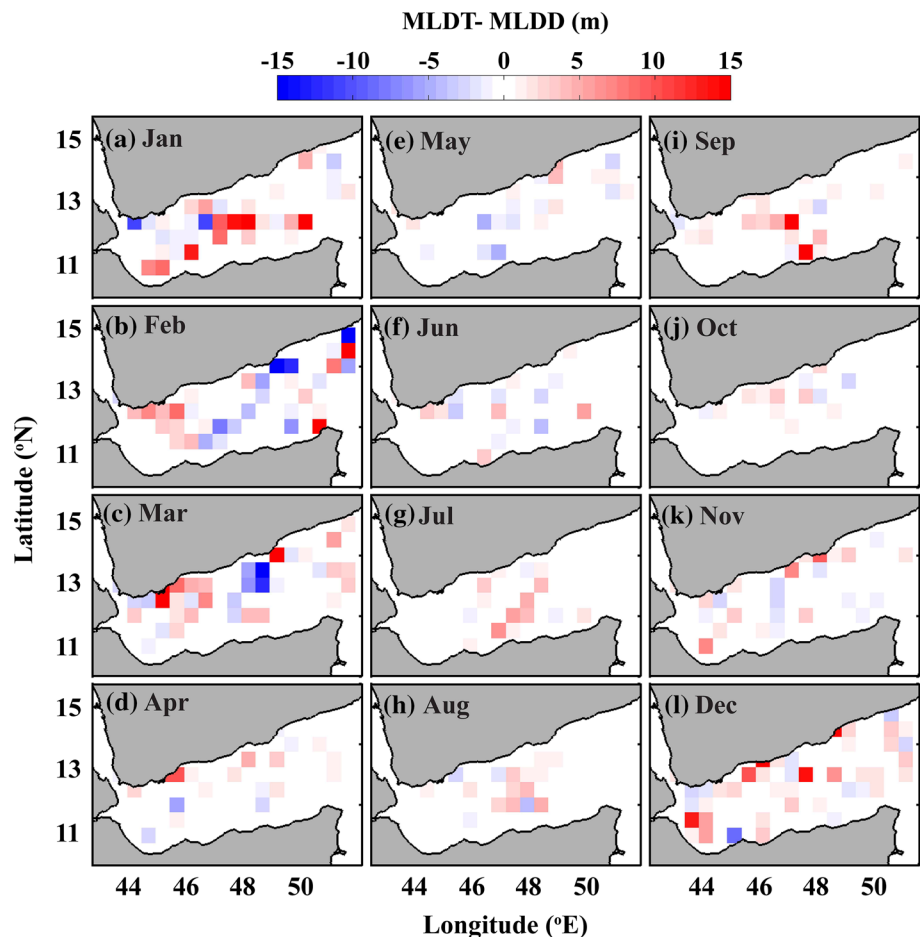


**Table 1** The monthly average MLDT-MLDD in the Gulf of Aden for the grids with salinity profiles

Month	MLDT (m)	MLDD (m)	MLDT-MLDD (m)
1	67.61	65.66	1.95
2	68.22	68.36	-0.14
3	40.32	39.11	1.20
4	22.70	22.10	0.60
5	18.13	18.50	-0.38
6	18.22	18.10	0.12
7	19.48	19.06	0.42
8	19.02	18.74	0.28
9	17.39	16.68	0.71
10	19.19	19.14	0.06
11	28.62	28.06	0.56
12	46.59	44.87	1.72

**Table 2** The monthly values of net heat flux and freshwater flux in the Gulf of Aden (spatially averaged)

Month	Net heat flux (W/m <sup>2</sup> )	Freshwater flux (mm/day)		
		<i>P</i>	<i>E</i>	<i>P-E</i>
1	-51.2	0.16	4.29	-4.13
2	-7.3	0.12	3.68	-3.56
3	40.5	0.26	3.19	-2.93
4	63.2	0.52	2.93	-2.41
5	53.4	0.6	2.83	-2.23
6	-76.7	0.33	3.98	-3.65
7	-100	0.49	4.55	-4.06
8	-32.2	0.85	3.91	-3.06
9	21.8	0.56	3.28	-2.72
10	-9.8	0.4	3.92	-3.52
11	-40	0.39	4.46	-4.07
12	-62.5	0.26	4.64	-4.38

western Gulf is warmer than the eastern Gulf throughout the year, with a larger difference from June to November. The MLT has two peaks, during May–June and September–October, probably due to the net heat gain from increase in short-wave radiation and decrease in evaporation (Table 2) during March–May and September, respectively.

**3.2 The influence of major forces**

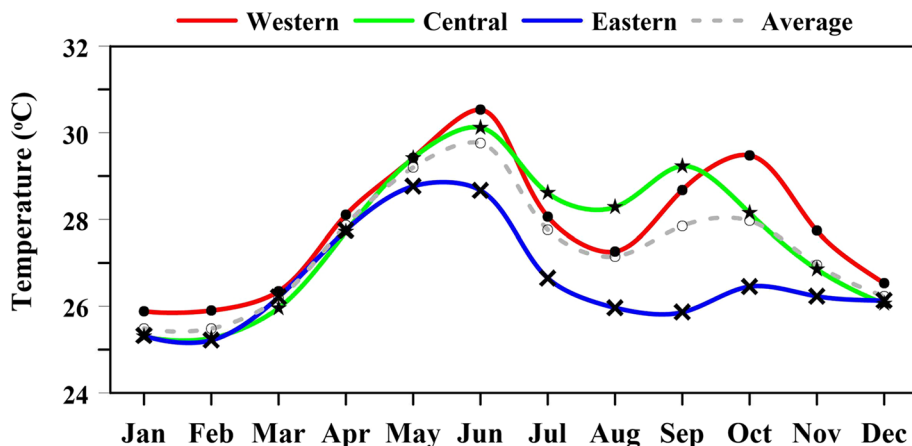
The depth of the mixed layer is predominantly controlled by the variation of net heat flux, the freshwater input and the wind stress. The net gain of heat at the ocean surface may strengthen the stratification and inhibit mixing, while the net loss of heat from the ocean may weaken the stratification, leading to increased mixing. The freshwater loss decreases the buoyancy and the stability, resulting in intensification of vertical mixing, whereas the freshwater gain increases both the buoyancy and the stability, leading to a stratified ocean with less mixing. The wind stress is one of

the primary dynamic forces generating the turbulence and the upper layer motion through the transfer of momentum. The shear and stirring generated by the surface wind stress enhance vertical mixing within the mixed layer.

**3.3 Net heat flux**

The annual cycle of heat exchange shows that the Gulf gains heat during March–May and September with heat loss in the remaining months. The monthly climatology of heat and freshwater flux is tabulated in Table 2. Apart from the expected heat loss during winter, it has been observed that the Gulf is losing heat during June–August. This is mainly due to enhanced evaporative heat loss associated with the relatively strong, hot and dry southwesterly winds from neighboring desert land blowing over the underlying warm surface water (Zhang et al. 2016), and the reduction in the incoming solar radiation due to

**Fig. 5** The monthly variability of MLT for the western, central and eastern Gulf of Aden



increase in cloudiness (Sultan and Ahmad 1997; Abualanaja et al. 2011).

The change in the MLT due to the net heat flux ( $\Delta MLT_Q$ ) is computed using the basic equation,

$$\Delta MLT_Q = \frac{Q}{(\rho h C_p)} \Delta t \tag{4}$$

where  $Q$  is surface net heat flux,  $\rho$  is average density of the mixed layer,  $h$  is the depth of the mixed layer,  $C_p$  is the specific heat of the water estimated based on average temperature and salinity of mixed layer from World Ocean Atlas 2013 (Locarnini et al. 2013; Zweng et al. 2013) and  $\Delta t$  is the time. The density is considered a constant of  $1023 \text{ kg m}^{-3}$ . The time tendency of MLT ( $\Delta MLT$ ) from in situ profiles is in reasonably good agreement with the variability of  $\Delta MLT_Q$  (Fig. 6). The temporal variability and magnitude of  $\Delta MLT$  is probably governed by the net heat flux in the Gulf.

The signature of temperature decrease (negative  $\Delta MLT_Q$ ) during June–August is not clearly visible in the MLD pattern. To check this, the static stability of the water column is calculated following Pond and Pickard (1983) as

$$E \approx \frac{1}{\rho} \frac{\partial \rho}{\partial z} \tag{5}$$

where  $\rho$  is the in situ density and  $z$  is the depth. The water column is considered stable if  $E > 0$ , neutral if  $E = 0$ , and unstable if  $E < 0$ . The static stability in the surface layer of 250 m in the Gulf is estimated based on Eq. 5, and the average stability during each month is shown in Fig. 7. The stability during June–August is two times stronger than that of winter. Therefore, even in the presence of heat loss from the surface, the mixed layer deepening is limited to a large extent. As a result, the signature of temperature decrease during June–August is not clearly visible in the MLD pattern.

### 3.4 Freshwater flux

The monthly average values of precipitation and evaporation are given in Table 2. The average freshwater input through precipitation in the Gulf is  $< 1 \text{ mm day}^{-1}$  throughout the year, while that of the evaporation is approximately 3–5 times greater than the precipitation. The minimum values of evaporation are observed during May and September. This is due to the weak surface winds in May and September associated with the reversal of wind direction. The mean wind speed for the months of May and September are respectively  $2.0 \text{ m s}^{-1}$  and  $1.6 \text{ m s}^{-1}$ , while it is greater than  $4 \text{ m s}^{-1}$  for the rest of the months. Further, the Gulf does not have any significant freshwater input through river discharge too. Due

**Fig. 6** The rate of time changes in the MLT obtained from the surface heat flux ( $\Delta MLT_Q$ ) and that obtained from the individual temperature profiles ( $\Delta MLT$ ) in the Gulf of Aden [ $\Delta MLT(\text{Feb}) = MLT(\text{Feb}) - MLT(\text{Jan})$ ]

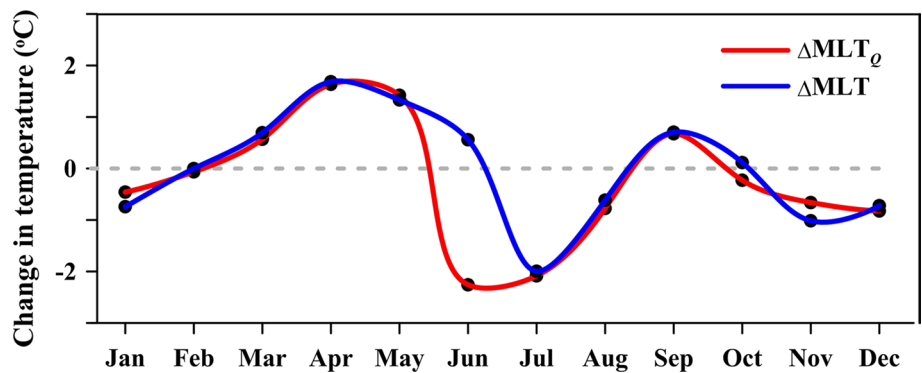
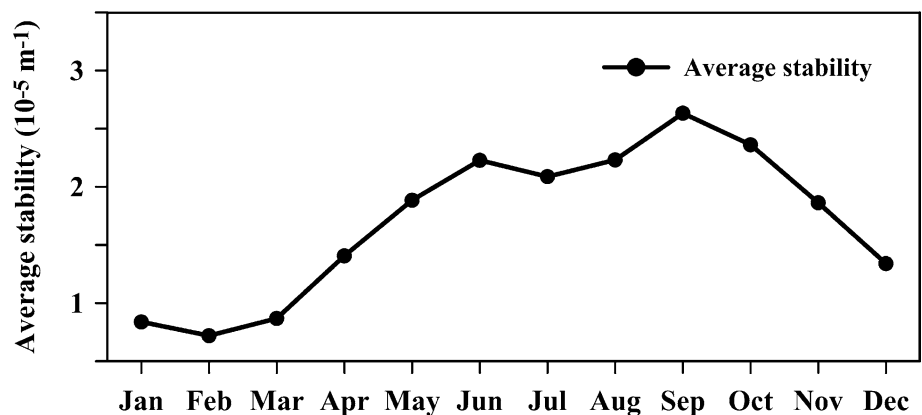


**Fig. 7** The monthly variability of static stability for a 0–250-m water column in the Gulf of Aden



to these reasons, the effect of freshwater flux on MLD variability is mostly associated with evaporation, which has a contribution of > 90% to the total freshwater flux.

The Gulf experiences a loss of freshwater throughout the year, with maximum loss centered in December and July, leading to densification of surface water and possible vertical mixing. During December, a deep MLD is visible, in agreement with the increased freshwater loss. However, during July, the signature of freshwater loss is not evident in the MLD because the mixing during this period is largely limited by the presence of already existing strong stratification.

### 3.5 Wind stress

The Gulf experiences a seasonally reversing wind system, with the north-easterly wind during winter and south-westerly wind during summer (Fig. 8). The reversal of wind direction from north-easterly to south-westerly takes place in May, and the opposite in September. The wind stress during winter and summer are relatively high in the south-central Gulf. Moreover, unlike that of winter, repeated high and low wind stress regions are visible along the southern Gulf during summer. The topography maps from ETOPO1 (<https://data.nodc.noaa.gov/cgi-bin/iso?id=gov.noaa.ngdc.mgg.dem:316> (Amante 2009)) revealed the presence of multiple mountain gaps along the southern coastal area. The winds

during summer are funneled to the Gulf through these mountain gaps. A similar wind stress pattern is reported by previous researchers also (Fratantoni et al. 2006; Yao and Hoteit 2015). This resulted in higher wind stress in the mountain gap regions and weak wind stress in the mountain-induced wind shadow areas.

The wind stress exerts turbulence in the surface layer and enhances the mixing process. The resultant changes in MLD are greatly dependent on the stratification in the surface layer, leading to stronger mixing in the least stratified conditions. Additionally, the associated Ekman transport leads to the deepening of the mixed layer in the northern Gulf and shoaling in the southern Gulf during winter, and nearly opposite pattern in summer. A detailed discussion on the wind-induced coastal Ekman upwelling/downwelling in the Gulf is provided in Sect. 3.4.

### 3.6 The impact of eddies

The Gulf is characterized by multiple eddies (Fratantoni et al. 2006; Alsaafani et al. 2007; Bower and Furey 2011; Zhai and Bower 2013) with basin-wide dimension. These eddies can considerably alter the hydrography of the Gulf. The XBT observations collected during two cruises, a winter cruise (from 20th to 21st January 2002) and a summer cruise (5th July to 7th August 2009), are shown in Fig. 9, along

**Fig. 8** The monthly climatology of the wind stress (shaded) and the wind direction (vectors) in the Gulf of Aden

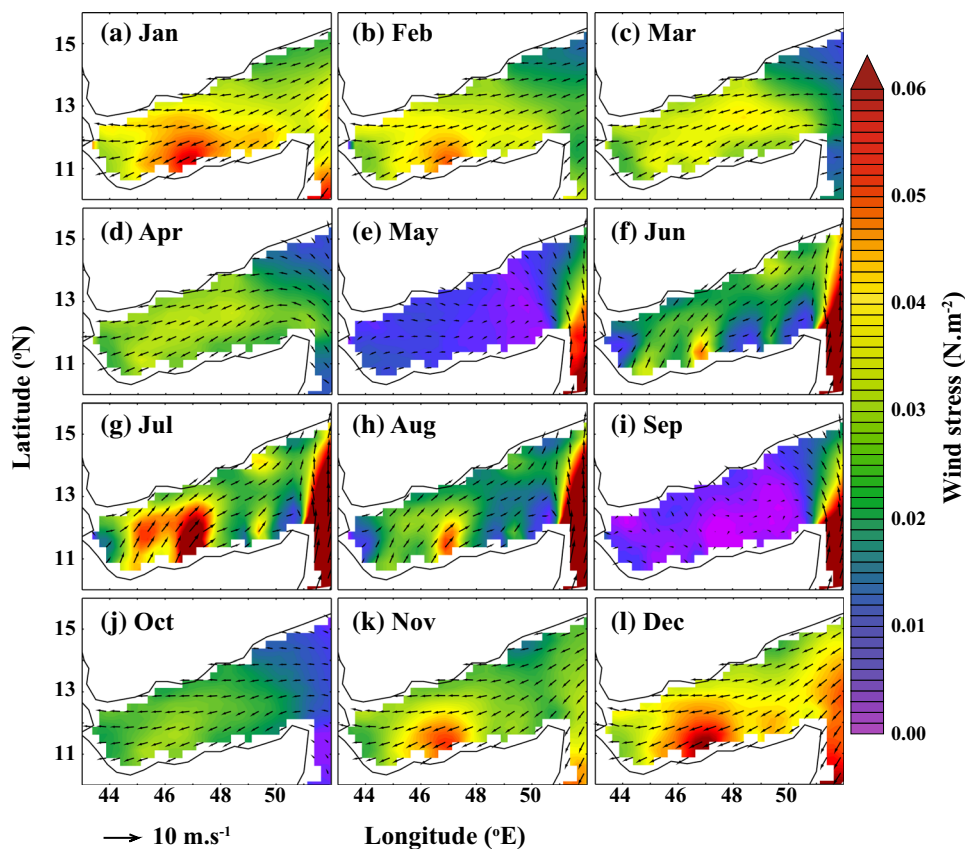
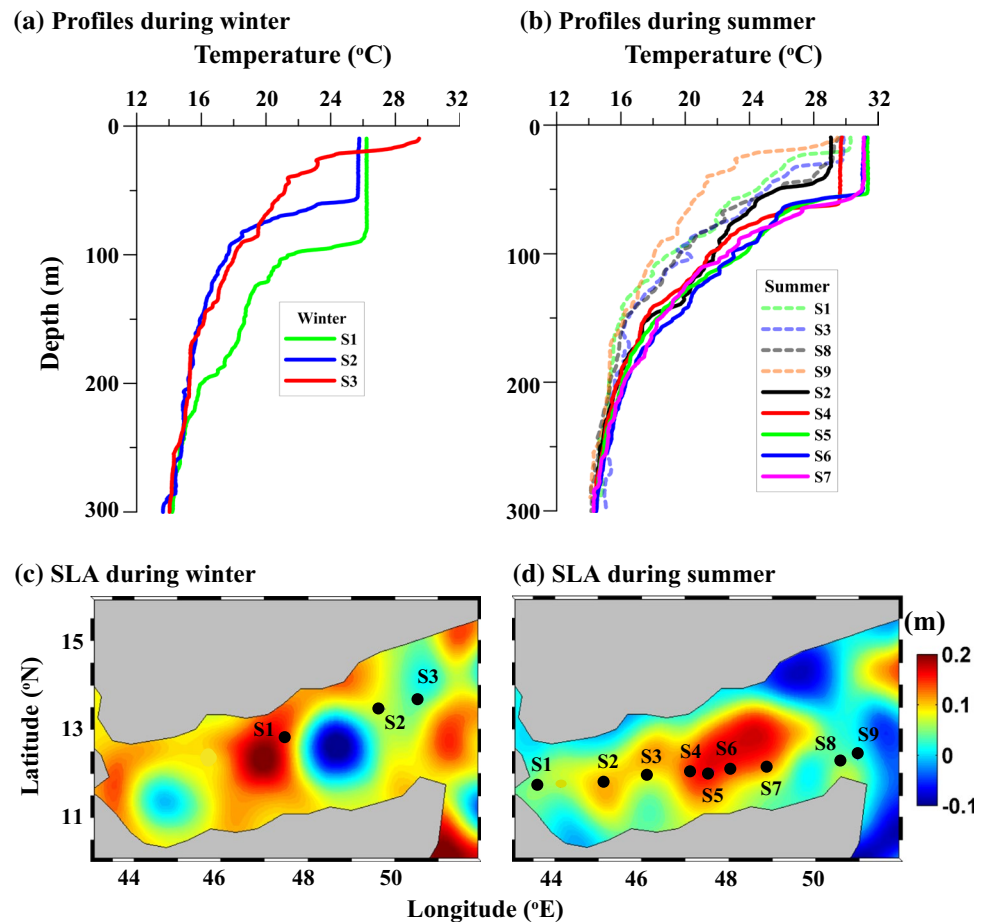




**Fig. 9** The temperature profiles collected during the two cruises: **a** a winter cruise (from 20th to 21st January 2002) and **b** a summer cruise (5th July to 7th August 2009). The SLA maps during the two cruises are shown in **c** and **d**, respectively



with the SLA maps averaged for approximately 1 week prior to the profiling time. Station S1 is located within an anticyclonic eddy and station S3 within a cyclonic eddy, while station S2 is outside both eddies (Fig. 9a, c). The mixed layer at S1 (S3) is significantly deeper (shallower) than the mixed layer at S2 due to the presence of an anticyclonic eddy (cyclonic eddy) (Fig. 9a, c). The presence of multiple eddies in winter significantly changed the mixed layer in the entire basin. Similarly, the anticyclonic eddy formed in the central Gulf during summer significantly deepens mixing in the central Gulf (at stations S4, S5, S6 and S7 in Fig. 9b, d). Station S2 is also located in an anticyclonic eddy, and the associated deepening is visible in the temperature profile.

The averaged SLA during peak winter (from 1st January to 28th February) and during peak summer (from 1st July to 31st August) for four consecutive years is shown in Fig. 10. The cyclonic and anticyclonic eddies during winter and the anticyclonic during summer are present in all the years, and most of them are basin-wide. The SLA confirms that eddies during summer are formed at the nearly same location every year, while those of winter are changing their location over time. Alsaafani et al. (2007) reported similar results, that the winter eddies are propagating in the westward direction,

while the summer eddy is continued in the central Gulf. Bower and Furey (2011) and Gittings et al. (2017) stated that the summer eddy is sustained in the central Gulf by the presence of a relatively strong negative wind stress curl and associated Ekman convergence.

The westward-moving eddies likely change the MLD of the region during its movement from east to west. In general, the cyclonic eddies result in shallower MLD, and anticyclonic eddies result in deeper MLD. The summer eddy, with well-defined anticyclonic circulation, and which is sustained in the central Gulf during July–August, makes the MLD in the central Gulf 40–50 m deeper than that in the eastern and western Gulf during summer. This eddy-induced deep MLD core develops in June, peaks in July and fades by September. The presence of eddies during winter is not clearly visible in the MLD climatology, due to the movement of eddies.

### 3.7 The north–south difference in MLD and upwelling

A nearly reversing MLD pattern is observed between the northern and the southern Gulf. The MLD over the northern Gulf is greater than the southern side during winter. This

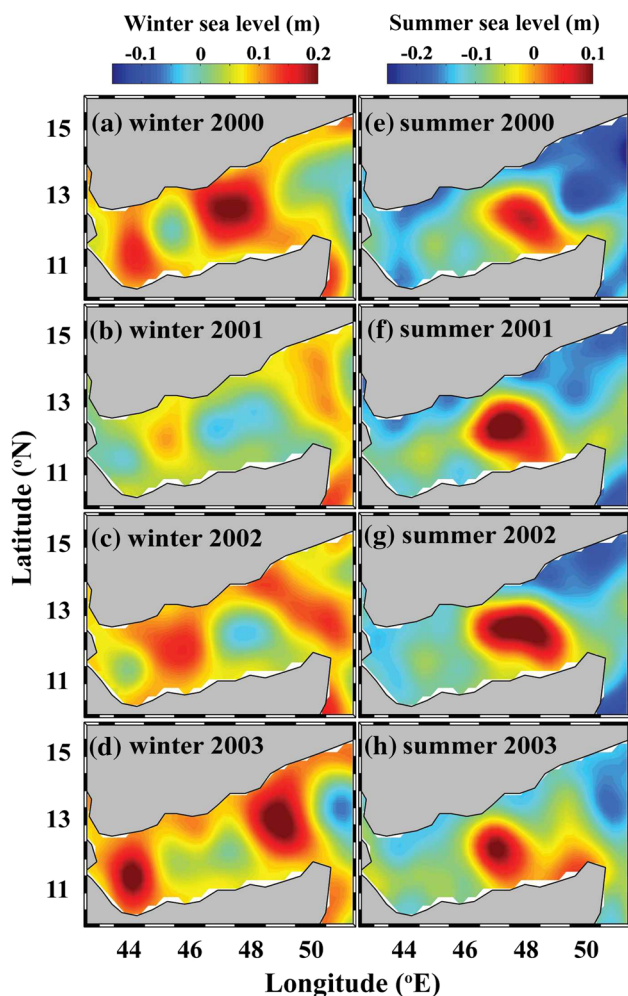


**Fig. 10** The average SLA maps for the years 2000, 2001, 2002 and 2003 in the Gulf of Aden during **a–d** winter and **e–h** summer

pattern reversed during summer when the MLD over the southern Gulf become greater than that of the northern Gulf. To show the north–south difference, two section lines are considered respectively along the north and southern Gulf (the section lines are marked in Fig. 1). The MLD of the northern Gulf is greater than the southern Gulf by approximately 10–20 m in December and January (Fig. 11). The difference gradually disappeared and reversed by June when the mixed layer in the southern Gulf becomes deeper than the northern Gulf. This pattern continued till August and gradually weakened by September. The north–south difference in MLD during winter is higher and widespread comparing to that of summer, largely due to the existing strong stratification in summer which inhibits vertical mixing to a great extent.

The prevailing northeasterly winds during October to April are mostly parallel to the northern and southern coast of the Gulf. Figure 11b shows the climatological along-coast wind component in the region. The along-coast component

of wind and the MLD difference are well correlated to each other (correlation coefficient = 0.7). The along-coast component of wind is negative from October to April (towards the western Gulf). This results in net Ekman transport to the northern Gulf and generates coastal Ekman upwelling along the southern coast and downwelling along the northern coast. The relatively strong wind system during June to August blows more or less parallel to the coast in the south-westerly direction due to the presence of coastal mountains. The along-coast component of wind is positive during this period (toward the eastern Gulf). This leads to a reverse phenomenon, where the net Ekman transport is towards the southern Gulf with coastal Ekman downwelling along the southern coast and upwelling along the northern coast.

The results shown in Fig. 11 are consistent with previous studies. The upwelling exists along the northern coast during summer with a favorable south-westerly wind system (Johns et al. 1999; Alsaafani 2008), and along the southern coast during winter with a favorable north-easterly wind system (Johns et al. 1999; Aiki et al. 2006; Alsaafani 2008; Alkawri and Gamoyo 2014; Yao and Hoteit 2015). The previous studies and the observed coastal Ekman upwelling pattern confirm that the observed north–south MLD variability shown in Fig. 11 is mainly due to the seasonally reversing wind system in the region and associated coastal Ekman upwelling/downwelling.

## 4 Summary and conclusions

The main theme of this work is to produce an MLD climatology in the Gulf of Aden and to understand the spatial and temporal variability of MLD. For the first time in the Gulf, a monthly climatology of MLD is derived from in situ temperature profiles with  $0.5^\circ \times 0.5^\circ$  resolution. The present work demonstrates the spatial and temporal variability of MLD in the Gulf and discusses the major physical processes linked to the mixed layer changes.

The winter deepening of the mixed layer began in November in the western Gulf, spread to a wider area in December, and peaked in January–February with a relatively deeper mixed layer in the western and northern Gulf. The increase in solar insolation and decrease in latent heat release from March to May lead to mixed layer shoaling in the Gulf, which is intensified due to the parallel development of strong stratification (Fig. 3). The shallowest mixed layer is observed in August for most of the area in the Gulf of Aden, except the south-central region. In the south-central region, a deep mixed layer core is noticed in the July–August period.

The heat exchange between the ocean and atmosphere significantly affects the MLD variability in the Gulf. As shown in Fig. 6, the variability of mixed layer temperature is probably governed by the net heat flux. The surface layer cooling

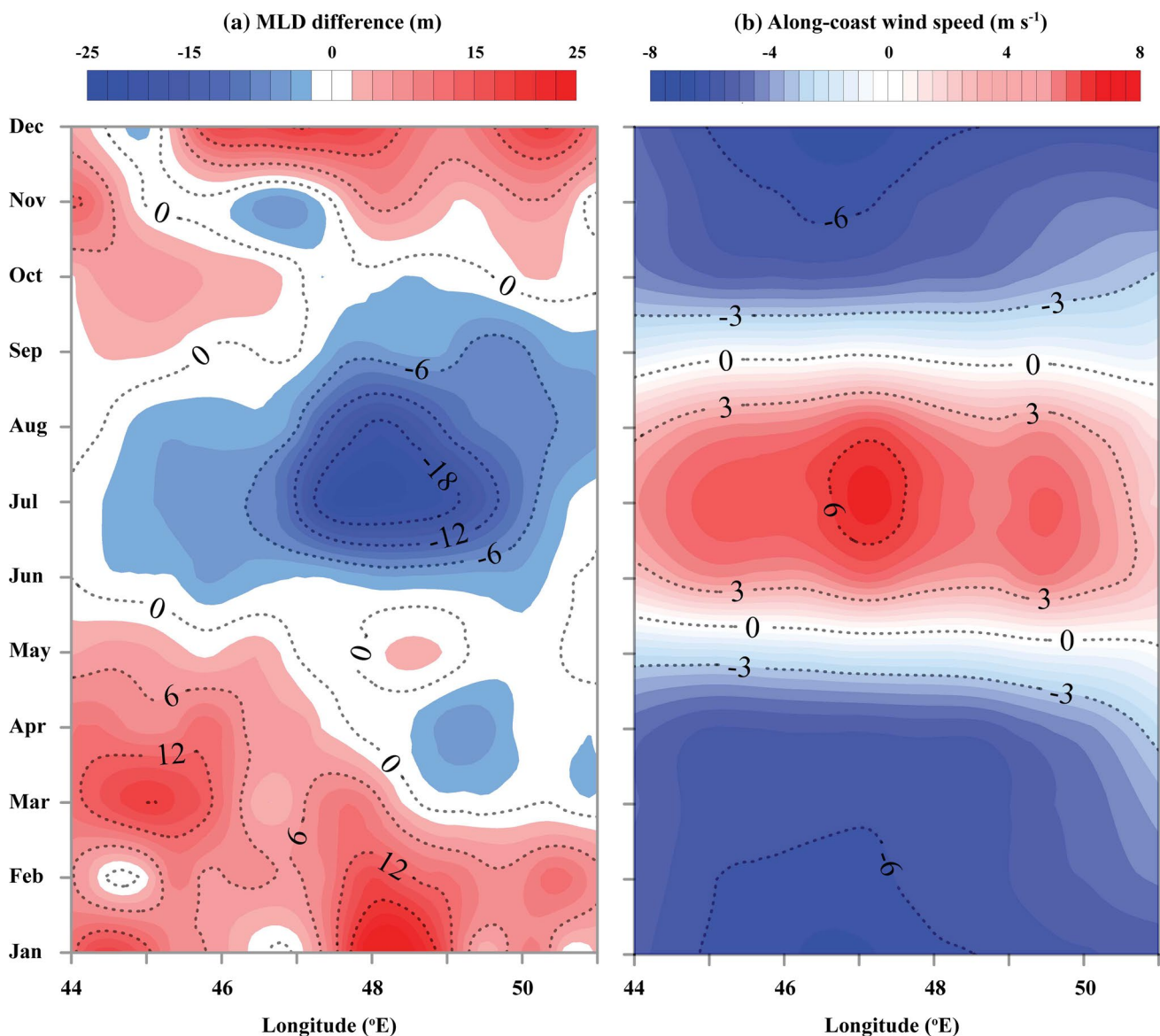


**Fig. 11** **a** The difference in MLD between the northern and the southern Gulf of Aden along the line shown in Fig. 1. **b** The mean along-coast component of wind in the Gulf (positive values denote the direction towards the eastern Gulf)

from November to January results in deepening of the mixed layer in the region. The heat loss during June–August did not cause considerable deepening of the mixed layer due to the already existing strong stratification in May. The freshwater flux in the Gulf of Aden is extensively dominated by the contribution from evaporation (> 90%). The region experience densification of surface water throughout the year from freshwater loss, with peak loss in December. The spatial and temporal variability observed in the MLD climatology has a complex MLD pattern, indicating the presence of other dominant dynamical processes like upwelling and eddies.

The upwelling/downwelling events along northern and southern coastal regions associated with the wind system

are evident in the MLD climatology (Figs. 3 and 11). The coastal Ekman downwelling and associated deepening of the mixed layer is witnessed in the northern Gulf during winter and in the southern Gulf during summer. Similarly, the coastal Ekman upwelling resulted in shallower MLD in the southern Gulf during winter and in the northern Gulf during summer.

Eddies are significantly varying the MLD structure in the Gulf of Aden. The cyclonic and anticyclonic eddies during winter, which are propagating in the westward direction, significantly change the MLD along its path. Similarly, the permanent anticyclonic eddy during summer in the central Gulf makes the MLD of the region greater than both eastern and



western basin. The signature of the summer eddy in the central Gulf is noticeable in the MLD climatology, while that of remaining eddies is not. The cyclonic and anticyclonic eddies during the remaining seasons are not permanently located in specific locations. Due to this effect, the localized signature of eddies is not visible in the climatological mixed layer.

The MLD variability in the Gulf can be summarized as follows. The influence of heat exchange leads to general northern-hemisphere MLD variability with winter deep and summer shallow mixed layers. The seasonally reversing wind system introduced additional north–south asymmetry in the MLD structure with a greater mixed layer in the northern Gulf during winter and in the southern Gulf during summer. Further complexity is generated by the presence of multiple eddies, which are present throughout the year. This jointly resulted in a very complex MLD pattern in the Gulf of Aden. The gridded MLD climatology, produced from in situ profiles, provides important details for the first time on MLD seasonality in the Gulf of Aden, and it is helpful in better understanding of upper-ocean physical and biological processes, including the distribution of heat and primary productivity. More salinity profiles are necessary for understanding the detailed mechanism of the mixed layer. Due to shortage of salinity profiles, in the present work, we use the MLDT to study MLD variability. A more detailed investigation can be done in the future with a significant number of salinity profiles.

**Acknowledgements** The authors acknowledge TropFlux, TRMM, AVISO, QuikSCAT, the World Ocean Database and Coriolis Data Center for making their data products publicly available. The authors also acknowledge the institutes who have provided CTD profiles from different cruises. The author CPA acknowledges the Deanship of Graduate Studies, King Abdulaziz University, Jeddah, for providing a Ph.D. fellowship. The new climatology of MLD is available from public data repository “Figshare” (<https://doi.org/10.6084/m9.figshare.5913397>). The data can be accessed after acceptance of this manuscript.

## References

- Abdulla CP, Alsaafani MA, Alraddadi TM, Albarakati AM (2016) Estimation of mixed layer depth in the Gulf of Aden: a new approach. *PLoS One* 11:e0165136. <https://doi.org/10.1371/journal.pone.0165136>
- Abdulla CP, Alsaafani MA, Alraddadi TM, Albarakati AM (2018) Mixed layer depth variability in the Red Sea. *Ocean Sci* 14(4):563–573. <https://doi.org/10.5194/os-14-563-2018>
- Abualanaja YO, Ahmad F, Al-Mtairi NA (2011) Balance of surface, advective and up-welling heat fluxes in the Gulf of Aden. *Indian J Mar Sci* 40:42–47
- Aiki H, Takahashi K, Yamagata T (2006) The Red Sea outflow regulated by the Indian monsoon. *Cont Shelf Res*. <https://doi.org/10.1016/j.csr.2006.02.0.17>
- Al Saafani MA, Shenoi SSC (2007) Water masses in the Gulf of Aden. *J Oceanogr* 63:1. <https://doi.org/10.1007/s10872-007-0001-1>
- Alkawri A, Gamoyo M (2014) Remote sensing of phytoplankton distribution in the Red Sea and Gulf of Aden. *Acta Oceanol Sin* 33:93–99. <https://doi.org/10.1007/s13131-014-0527-1>
- Alsaafani MA (2008) Physical oceanography of the Gulf of Aden. PhD thesis, Goa Univ 207
- Alsaafani MA, Shenoi SSC, Shankar D et al (2007) Westward movement of eddies into the Gulf of Aden from the Arabian Sea. *J Geophys Res* 112:C11004. <https://doi.org/10.1029/2006JC004020>
- Amante C (2009) ETOPO1 1 arc-minute global relief model : procedures, data sources and analysis. Boulder, Colo. : US Dept. of Commerce, National Oceanic and Atmospheric Administration, National Environmental Satellite, Data, and Information Service, National Geophysical Data Center, Marine Geology and Geophysics Division, [2009]
- Bower AS, Furey HH (2011) Mesoscale eddies in the Gulf of Aden and their impact on the spreading of Red Sea outflow water. *Prog Oceanogr* 96:14–39. <https://doi.org/10.1016/j.pcean.2011.09.003>
- Boyer TP, Levitus S (1994) Quality control and processing of historical temperature, salinity, and oxygen data. NOAA Tech Rep NESDIS 81:65
- Boyer TP, Antonov JI, Baranova OK, et al (2013) World Ocean Database 2013, NOAA Atlas NESDIS 72, S. Levitus, Ed., A. Mishonov, Technical Ed. Silver Spring
- Cabanes C, Grouazel A, von Schuckmann K et al (2013) The CORA dataset: validation and diagnostics of in situ ocean temperature and salinity measurements. *Ocean Sci* 9:1–18. <https://doi.org/10.5194/os-9-1-2013>
- Chen D, Busalacchi AJ, Rothstein LM (1994) The roles of vertical mixing, solar radiation, and wind stress in a model simulation of the sea surface temperature seasonal cycle in the tropical Pacific Ocean. *J Geophys Res* 99:20345. <https://doi.org/10.1029/94JC01621>
- Cheng L, Zhu J, Cowley R et al (2014) Time, probe type, and temperature variable bias corrections to historical expendable bathythermograph observations. *J Atmos Ocean Technol* 31:1793–1825. <https://doi.org/10.1175/JTECH-D-13-00197.1>
- Currie RI, Fisher AE, Hargraves PH (1973) Arabian Sea upwelling. Springer Verlag, Berlin
- D’Ortenzio F, Iudicone D, de Boyer Montégut C et al (2005) Seasonal variability of the mixed layer depth in the Mediterranean Sea as derived from in situ profiles. *Geophys Res Lett* 32:1–4. <https://doi.org/10.1029/2005GL022463>
- de Boyer Montégut C, Madec G, Fischer AS et al (2004) Mixed layer depth over the global ocean: An examination of profile data and a profile-based climatology. *J Geophys Res C Ocean* 109:1–20. <https://doi.org/10.1029/2004JC002378>
- Ducet N, Le Traon PY, Reverdin G (2000) Global high-resolution mapping of ocean circulation from TOPEX/Poseidon and ERS-1 and -2. *J Geophys Res Ocean* 105:19477–19498. <https://doi.org/10.1029/2000JC900063>
- Fratantoni DM, Bower AS, Johns WE, Peters H (2006) Somali Current rings in the eastern Gulf of Aden. *J Geophys Res Ocean*. <https://doi.org/10.1029/2005jc003338>
- Gittings JA, Raitso DE, Racault MF et al (2017) Seasonal phytoplankton blooms in the Gulf of Aden revealed by remote sensing. *Remote Sens Environ* 189:56–66. <https://doi.org/10.1016/j.rse.2016.10.043>
- Huffman GJ, Adler RF, Bolvin DT et al (2007) The TRMM Multi-satellite precipitation analysis: quasi-global, multi-year, combined-sensor precipitation estimates at fine scale. *J Hydrometeorol* 8:38–55
- J-DOSS JODC (2003) Japan Oceanographic Data Center J-DOSS: JODC data on-line service system
- Johns WE, Jacobs GA, Kindle JC et al (1999) Arabian marginal seas and gulfs. University of Miami RSMAS Technical Report. University of Miami, Florida, USA



- Kabanova JG (1968) Primary production of the northern part of the Indian Ocean. *Oceanology* 8:214–225
- Kara AB, Rochford PA, Hurlburt HE (2003) Mixed layer depth variability over the global ocean. *J Geophys Res* 108:3079. <https://doi.org/10.1029/2000JC000736>
- Keerthi MG, Lengaigne M, Drushka K et al (2016) Intraseasonal variability of mixed layer depth in the tropical Indian Ocean. *Clim Dyn* 46:2633–2655. <https://doi.org/10.1007/s00382-015-2721-z>
- Le Traon PY, Dibarboure G (1999) Mesoscale mapping capabilities of multiple-satellite altimeter missions. *J Atmos Ocean Technol* 16:1208–1223. [https://doi.org/10.1175/1520-0426\(1999\)016%3c1208:MMCOMS%3e2.0.CO;2](https://doi.org/10.1175/1520-0426(1999)016%3c1208:MMCOMS%3e2.0.CO;2)
- Lim S, Jang CJ, Oh IS, Park J (2012) Climatology of the mixed layer depth in the East/Japan Sea. *J Mar Syst* 96–97:1–14. <https://doi.org/10.1016/j.jmarsys.2012.01.003>
- Locarnini RA, Mishonov AV, Antonov II, Boyer TP, Garcia HE, Baranova OK, Zweng MM, Paver CR, Reagan JR, Johnson DR, Hamilton M (2013) World ocean atlas 2013. Volume 1, Temperature. Levitus S, Mishonov A (eds) NOAA Atlas NESDIS 73, 40 pp. <https://doi.org/10.7289/v55x26vd>
- Lorbacher K, Dommenges D, Niiler PP, Köhl A (2006) Ocean mixed layer depth: a subsurface proxy of ocean-atmosphere variability. *J Geophys Res Ocean* 111:1–22. <https://doi.org/10.1029/2003JC002157>
- Murray SP, Johns W (1997) Direct observations of seasonal exchange through the Bab el Mandab Strait. *Geophys Res Lett* 24:2557–2560. <https://doi.org/10.1029/97GL02741>
- Polovina J, Mitchum GT, Evans T (1995) Decadal and basin-scale variation in mixed layer depth and the impact on biological production in the Central and North Pacific, 1960–88. *Deep Sea Res* 42:1701–1716
- Pond S, Pickard GL (1983) *Introductory physical oceanography*. Pergamon, Oxford
- Praveen Kumar B, Vialard J, Lengaigne M et al (2012) TropFlux: air-sea fluxes for the global tropical oceans—description and evaluation. *Clim Dyn* 38:1521–1543. <https://doi.org/10.1007/s00382-011-1115-0>
- Smeed DA (1997) Seasonal variation of the flow in the strait of Bab al Mandab. *Ocean Acta* 20:773–781
- Sultan SAR, Ahmad F (1997) Heat budget of the Gulf of Aden: surface, advective and upwelling heat fluxes. *Oceanol Acta* 20:665–672
- Sutton PJ, Worcester PF, Masters G et al (2014) Ocean mixed layers and acoustic pulse propagation in the Greenland Sea. *J Acoust Soc Am* 94:1517–1526. <https://doi.org/10.1121/1.408130>
- Terry P (1994) An evaluation of climatological data in the Indian Ocean area. *J Meteorol Soc Jpn* 3(72):359–386
- Wackernagel H (1998) *Multivariate Geostatistics*, 2nd edn. Springer-Verlag, New York
- Wentz FJ, Smith DK (2005) Remote sensing systems seawinds monthly ocean vector winds on 0.25 deg grid, Version 3a. Remote Sensing Systems, Santa Rosa, CA
- Yao F, Hoteit I (2015) Thermocline regulated seasonal evolution of surface chlorophyll in the Gulf of Aden. *PLoS One* 10:1–11. <https://doi.org/10.1371/journal.pone.0119951>
- Zhai P, Bower AS (2013) The response of the Red Sea to a strong wind jet near the Tokar Gap in summer. *J Geophys Res Ocean* 118:422–434. <https://doi.org/10.1029/2012JC008444>
- Zhang Q, Yang K, Shi Y (2016) Spatial and temporal variability of the evaporation duct in the Gulf of Aden. *Tellus Ser A Dyn Meteorol Oceanogr* 68:45. <https://doi.org/10.3402/tellusa.v68.29792>
- Zweng MM, Reagan JR, Antonov I, Locarnini RA, Mishonov AV, Boyer TP, Garcia HE, Baranova OK, Johnson DR, Seidov D, Biddle MM (2013) World ocean atlas 2013. Volume 2, Salinity. Levitus S, Mishonov A (eds) NOAA Atlas NESDIS 74, 39 pp. <https://doi.org/10.7289/V5251G4D>